

# Optical Variability of Hercules X-1/HZ Herculis

Matthias Aicher

supervised by Prof. Dr. Jörn Wilms, Dr. Remeis Sternwarte, Universität Erlangen

(Dated: March, 2007)

In this project the optical variability of the binary Hercules X-1/HZ Herculis is studied. Optical observations made in June, 2001 at the McDonald Observatory were analyzed with Fourier methods and in 4 of the approximately 50 runs optical pulsations near the neutron star's spin frequency were detected. The pulsed fraction varies from 0.8 to 1.2 % and is correlated with the orbital phase. It is shown that the frequency of the pulses is hardly Doppler-shifted and hence the pulses cannot be emitted by the accretion disc of Hercules X-1. Instead the surface of HZ Herculis seems to emit optical pulses due to the X-ray heating. A purely geometrical model of the binary is presented, that calculates the optical flux emitted by HZ Herculis taking into account the periodic X-ray heating through Hercules X-1. The model qualitatively describes the correlation of the pulsed fraction with the orbital phase.

## I. INTRODUCTION

The aim of this project is to investigate the optical variability of the eclipsing X-ray pulsar binary Hercules X-1/HZ Herculis. Hercules X-1 is a neutron star of 1.4 solar masses with a spin period of 1.24 s. Its companion star, HZ Herculis, is a variable star of about 2 solar masses (see [2]).

In the X-ray regime the variability of Hercules X-1 has been very well studied. So in this project we are only interested in the optical variability of the binary.

The X-ray pulses from Hercules X-1 also hit its nearby companion, which leads to a periodic heating of its atmosphere. So the question is: Does this periodic heating lead to a variability of the optical radiation emitted by HZ Herculis? In the 1970s Davidsen *et al.* first discovered optical pulses in the spectrum of HZ Herculis (see [3], [4]) and Middleditch *et al.* later confirmed those results (see [5], [6])

To investigate this problem we will make use of the powerful algorithm of the Fast Fourier Transform (FFT). So I will first introduce the basic principles of Fourier transforms and the algorithm for transforming discretely sampled data (section II). Afterwards I will give the properties of the binary Hercules X-1/HZ Herculis and present some earlier results on X-ray and optical variabilities (35d and 1.7d cycle).

In section IV results obtained from the optical observations at McDonald Observatory in June, 2001 are presented. We will use Fourier methods to study the *power spectral density* (PSD) of the recorded light curves and to determine possible pulsation frequencies. We will find that the presence of pulsed light depends on the orbital phase (1.7d cycle) of the binary. To explain this dependence a simple model for the reprocessing of X-rays on the surface of HZ Herculis is presented in section V.

## II. FAST FOURIER TRANSFORM

### A. General Properties

Some general properties of the Fourier transform are presented here. The whole theory of Fourier transforms and its numerical implementation was described by Press *et al.* (see [1]).

In our investigation we are dealing with counting rates, i.e. the number of photons detected per time interval  $dt$ . Since the rate is not constant, in general the counting rate is given as a function of time  $f(t)$ . But we are interested in the variability of the light curve and the characteristic periods for such variations. So we have to make a transition from the time domain to the frequency domain, which is given by the general Fourier transform:

$$\begin{aligned} H(f) &= \int_{-\infty}^{\infty} h(t)e^{2\pi ift} dt \\ h(t) &= \int_{-\infty}^{\infty} H(f)e^{-2\pi ift} df \end{aligned} \quad (1)$$

The function  $H(f)$  gives the amplitude as a function of the frequency  $f$ . It is in general a complex number, since it also contains the phase.

For our purpose it is more reasonable to consider the power contained in a frequency interval  $df$  than the complex amplitude. Therefore we define the *one-sided power spectral density* (PSD) for positive frequencies  $f$  as

$$P_h(f) = |H(f)|^2 + |H(-f)|^2. \quad (2)$$

Another useful tool for spectral analysis is the convolution of two functions  $f(t)$  and  $g(t)$ , which is defined as

$$g \star h = \int_{-\infty}^{\infty} g(\tau)h(t - \tau)d\tau \quad (3)$$

For the Fourier transform the *Convolution Theorem* holds

$$g \star h \Leftrightarrow G(f)H(f) \quad (4)$$

We will make use of this treatment to study the shape of the observed pulses in section IV, where we fold the observed light curves with a sine function of the significant frequency.

## B. Discrete Fourier Transform

Until now we have assumed that  $f(t)$  is a continuous analytic function, but our observation data is sampled at evenly spaced time intervals  $\Delta t$ . For  $N$  data samples we can produce only  $N$  independent numbers of output, i.e. we calculate the Fourier transform at the frequency values

$$f_n = \frac{n}{N\Delta t}, \quad n = -\frac{N}{2}, \dots, \frac{N}{2} \quad (5)$$

It can easily be seen that the frequency range is limited by the so called *Nyquist critical frequency*  $f_c = \frac{1}{2\Delta t}$ . For a given number of data samples it is not possible to resolve higher frequencies in the frequency domain than  $f_c$ .

To calculate the amplitudes for the discrete frequency values we have to replace the integral in (1) by a sum over the  $N$  data points

$$H(f_n) = \int_{-\infty}^{\infty} h(t)e^{2\pi i f_n t} dt \rightarrow \Delta t \sum_{k=0}^{N-1} h_k e^{2\pi i k n / N} \quad (6)$$

For the inverse Fourier transform it holds

$$h_k = \frac{1}{N} \sum_{n=0}^{N-1} H_n e^{-2\pi i k n / N} \quad (7)$$

## C. Fast Fourier Transform

Since we are dealing with a huge number of data samples (i.e. a huge  $N$ ), we are interested in finding a fast algorithm to calculate Fourier transforms.

Let us first consider the discrete Fourier transform given in eq. (6). Define a  $N \times N$ -matrix

$$A_{nk} = W^{nk} \quad (8)$$

with the complex number  $W = e^{2\pi i / N}$ . Then the discrete Fourier transform (6) can be written as a matrix multiplication

$$H_n = \sum_{k=0}^{N-1} A_{nk} h_k, \quad (9)$$

which requires  $N^2$  multiplications. The discrete Fourier transform is therefore an  $O(N^2)$  process. For our purpose this result is really deceiving, because we have to include many data points to obtain a good resolution in the frequency domain.

A class of more efficient algorithms are the so called *Fast Fourier Transforms (FFT)*. The most common of

these is the Cooley-Tukey algorithm, which will be presented here.

We restrict ourselves to the case, where  $N$  is a power of 2 (for spectral analysis we will only use numbers of segments, which fulfill this condition). The Basic idea is to split up a discrete transform of length  $N$  into a sum of two Fourier transforms of length  $N/2$ .

$$\begin{aligned} H_k &= \sum_{j=0}^{N-1} h_j e^{2\pi i j k / N} \\ &= \sum_{j=0}^{N/2-1} h_{2j} e^{2\pi i (2j)k / N} + \sum_{j=0}^{N/2-1} h_{2j+1} e^{2\pi i (2j+1)k / N} \\ &= \sum_{j=0}^{N/2-1} h_{2j} e^{2\pi i j k / (N/2)} + W^k \sum_{j=0}^{N/2-1} h_{2j+1} e^{2\pi i j k / (N/2)} \\ &= H_k^e + W^k H_k^o \end{aligned} \quad (10)$$

The first term consists of the even numbered samples, the second of the odd numbered. This is the so called *Danielson-Lanczos lemma*. It is obvious that we can apply this lemma recursively ( $H_k^e = H_k^{ee} + W^k H_k^{eo}$ ) until we have split up  $H_k$  into a sum of transforms of length 1, which is nothing but the identity applied to the input value. So it takes  $\log_2 N$  steps to arrive at the one point transforms  $H_k^{eee\dots}, H_k^{oee\dots}, H_k^{eoe\dots}, \dots$ . Each of these one point transforms corresponds to one input number  $f_n$ . To find out, which pattern of  $e$ 's and  $o$ 's corresponds to which  $n$ , one has to reverse the pattern of  $e$ 's and  $o$ 's, let  $e = 0$  and  $o = 1$ , and what you get is the value of  $n$  in binary (This procedure is called *bit reversal* and is described in detail in [1]).

Since we have to run through this procedure  $N$  times ( $N$  different values of  $k$ ), the FFT appears to be an  $O(N \log_2 N)$  process. To transform the lightcurves we use about  $10^5$  data points, so the difference between  $N^2$  and  $N \log_2 N$  is really enormous.

## III. THE SYSTEM HERCULES X-1/HZ HERCULIS

### A. General Information

The system HZ Herculis was discovered in 1936 and labeled as a classical variable star (Hoffmeister, 1941). In 1972 the system gained a big degree of popularity, when Tananbaum *et al.* identified the system as an eclipsing binary system containing the X-ray source Hercules X-1 during an observation with UHURU.

Shortly after this discovery, HZ Herculis was identified as the optical counterpart of Hercules X-1. These two stars rotate in an almost circular orbit with a period of 1.7 d. The inclination angle of the orbital plane is  $i = 83^\circ$ , i.e. we see the system almost edge on and we can observe periodical eclipses of Hercules X-1 by HZ Herculis.

TABLE I: Parameters of Hercules X-1/HZ Herculis (all values from Kuster [2])

System parameters		
Distance	$D$	$6.6 \pm 0.4$ kpc
Binary Orbital Period	$P_{orb}$	1.7003(3) d
Projected Orbital Radius	$a \cdot \sin i$	13.1902(9) s
Orbit inclination	$i$	$83(4)^\circ$
Eccentricity	$e$	$< 1.3 \times 10^{-4}$
Hercules X-1		
Mass	$M_x$	$1.5 \pm 0.3 M_\odot$
Spin Period	$P_{Spin}$	1.23781755 s
Magnetic Field Strength	$B$	$4.1 \times 10^{12}$ G
X-ray Luminosity	$L_x$	$3 \times 10^{37}$ erg/s
HZ Herculis		
Mass	$M_{opt}$	$2.3 \pm 0.3 M_\odot$
Radius	$R_{opt}$	$4.2 \pm 0.2 R_\odot$
Apparent Magnitude	$m_b$	13.2 – 14.7 mag

Another astonishing variability on long time scales is the 35d periodicity of the X-ray radiation. But this will not be discussed here, since the optical features are hardly affected by this periodicity. An investigation of this variability can be found in [2]. An overview on the system's parameters is presented in table I.

## B. Optical Variability of HZ Herculis

The optical counterpart of Hercules X-1, the variable HZ Herculis, shows variabilities on different time scales.

First the luminosity of the star changes strongly with a period of 1.7 days. This is due to the orbital motion of the binary. The X-ray radiation hitting HZ Herculis is reprocessed to optical wavelength, i.e. the X-ray heated side of HZ Herculis pointing towards Hercules X-1 shows a much greater luminosity than the 'back' of the star. Since we see the system almost edge-on, the optical flux received from HZ Herculis changes strongly with the orbital phase. We define phase 0 as the X-ray eclipse, i.e., at phase 0.5 we observe the highest luminosity.

This effect leads to a change of luminosity of about 1.6 mag during one orbital period (see Fig. 1)

Of course the X-ray pulsar does not emit radiation continuously. Instead the radiation is pulsed with a period of about 1.24 s. This phenomenon can be described by the lighthouse model. The X-ray radiation is emitted near the magnetic poles of the neutron star. Since the magnetic and the rotation axis of the pulsar are misaligned, an observer only detects radiation once each rotation. So the period of the pulses is simply the rotation period of the neutron star. I. e. HZ Herculis is heated periodically by Hercules X-1, which leads to optical pulsations. Observations of these optical pulsations were first reported by Davidsen *et al.* [3] and later confirmed by the long-

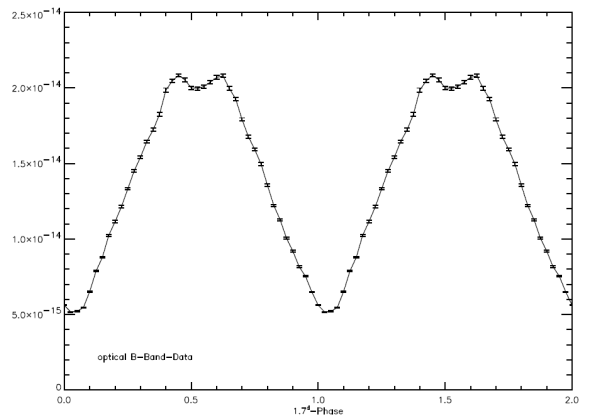


FIG. 1: Optical luminosity of HZ Herculis during the 1.7d cycle (Picture from Kuster [2])

term observations of Middleditch & Nelson [5]. But until now there have also been a lot of negative searches for pulsations in the light curve of HZ Herculis, so the results from the seventies could not be confirmed so far.

In this project I focused on searching for these optical pulsations in the observed light curves.

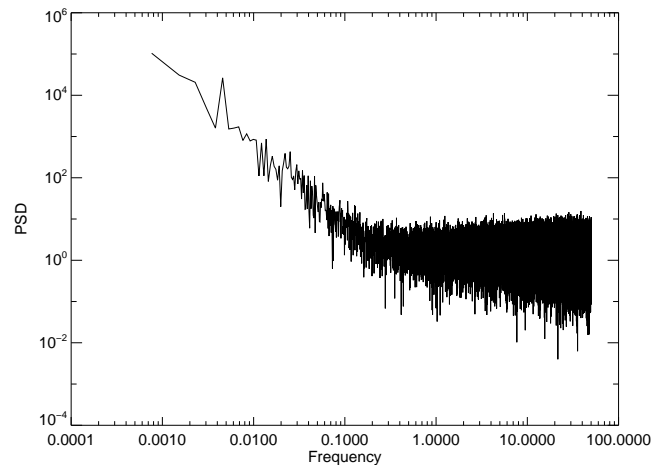


FIG. 2: PSD of a run from June 26, 2001 (U filter)

## IV. OBSERVATIONS

### A. Photometric Data

The binary Her X-1 was observed on 15 nights in June 2001 at the McDonald Observatory by M. Kuster and K. O'Brien. The data were taken by the P45 photometer. Counting rates were recorded in 10 ms intervals. The mean counting rate was about 5000 photons per second. For each night up to 7 runs of 4000 s were made. Therefore 5 different filters were used (B, C, R, U, V). Besides

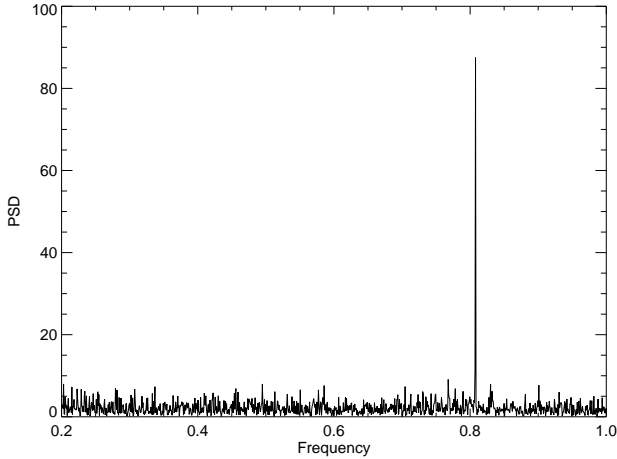


FIG. 3: PSD of the run from June 17, 04:34:07 - 05:40:47, U filter

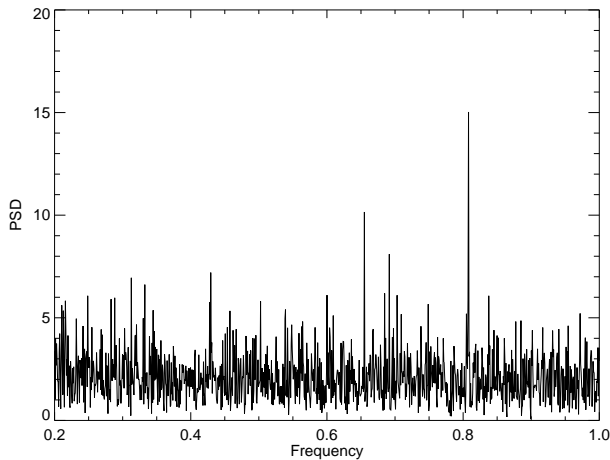
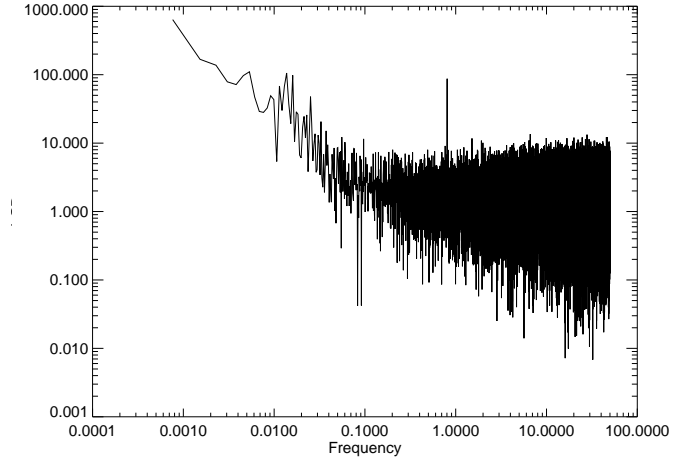
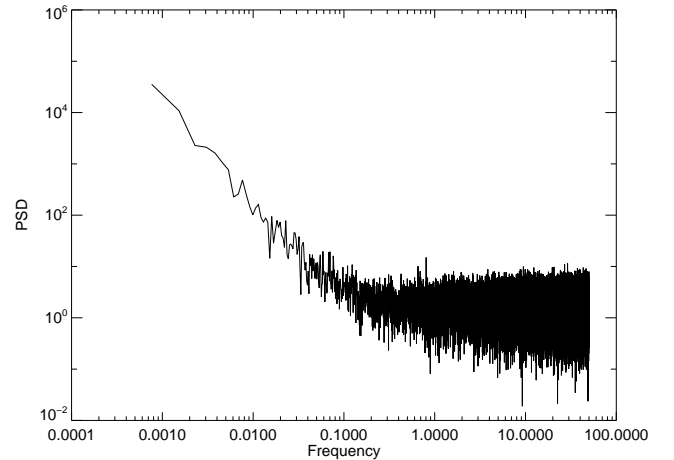


FIG. 4: PSD of the run from June 21, 06:43:12 - 07:49:52, U filter



a short observation of the optical background followed each run. These background light curves are necessary to determine, whether external influences are present.

## B. Data Analysis

As mentioned above we focus on searching for pulsation in the optical radiation of HZ Herculis that correspond to the pulses of the nearby neutron star Hercules X-1. In order to find pulsations in the observed light curves it is necessary to Fourier transform the sampled data to the frequency domain and calculate the PSD. If the light curve shows variability, we will find a peak in the PSD at the respective frequency.

To analyze the data we used the *Cooley-Tukey FFT* algorithm described in section II. Since the data for each run of 4000 s is sampled in 10 ms intervals, the *Nyquist*

*critical frequency* in our case is

$$f_c = \frac{1}{2\Delta t} = 50s^{-1}. \quad (11)$$

When calculating the PSD we used  $N = 2^{17} = 131072$  segments, i.e the resolution in the frequency domain is given by

$$\Delta f = \frac{f_c}{N/2} = 7.63 \times 10^{-4}s^{-1}. \quad (12)$$

In Fig. 2 the PSD of a typical light curve of HZ Herculis is shown on a double logarithmic scale. The high power at small frequencies is due to *red noise*. The spectral density of red noise is proportional to  $1/f^2$ , which describes the power law behavior of the PSD for small frequencies very well. For higher frequencies the mean power is constant and about 2. This number is due to the special normalisation chosen, called *Leahy*-normalisation (it is described in detail in [9]). That PSD does not in-

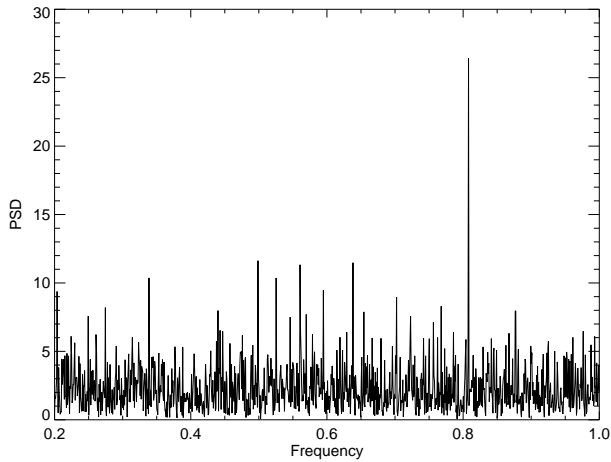


FIG. 5: PSD of the run from June 21, 07:54:20 - 09:01:00, U filter

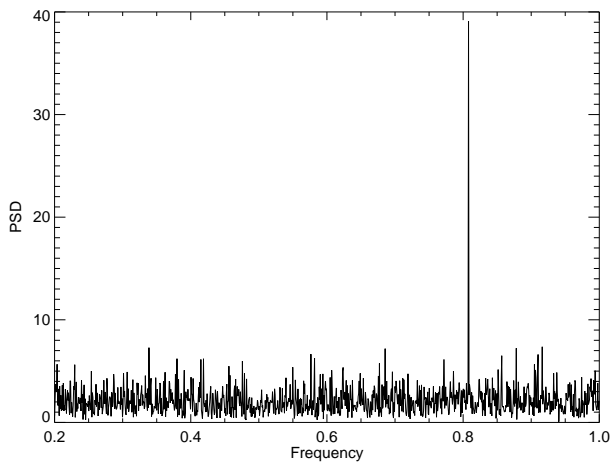
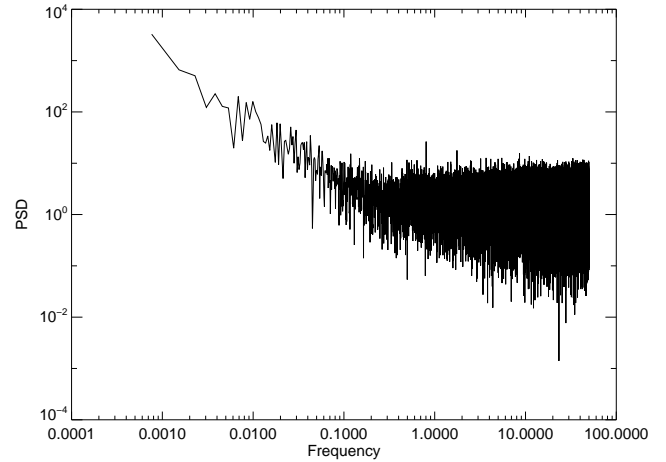
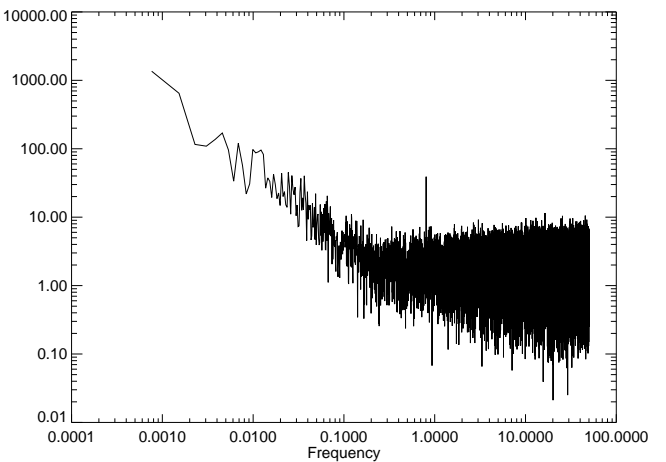


FIG. 6: PSD of the run from June 22, 04:25:41 - 05:32:21, U filter



indicate any variability, since no frequency gives a significantly high contribution to the PSD. Of course we expect high contributions only near the pulsation frequency of the neutron star.

Significant powers in that range were observed on 4 runs in 3 different nights. The PSDs of that light curves are shown in Fig. 3 to Fig. 6. All the shown plots are obtained from light curves from the U filter. But the resulting PSD is not filter dependent, i.e. the light curves from the other filters also show variability with the same period.

To exclude any external fluctuations that could produce 'artificial' variabilities, e.g. by the optics of the telescope itself or by other objects in the field of vision, the optical background was also analyzed with Fourier methods. For example the background PSD of the run from Fig. 3 is plotted in Fig. 9. One can easily see that no variability is present in the background light curve, i.e. the high power near the pulsation frequency must originate from the System Hercules X-1/HZ Herculis and is

not due to any external influence. The same holds for the background of the other light curves.

Now, that we know that the variability comes from the binary system, we still have to verify that the optical pulsation is due to reprocessed X-rays on the surface of HZ Herculis, because the pulsed light could also be emitted in the accretion disc of Hercules X-1.

Therefore we have to determine the significant frequencies more precisely. A way to do this is the so called *epoch folding*. The light curve is folded on the distinct period and the mean squared deviation ( $\chi^2$ ) of the resulting counting rate is calculated. This procedure is done for evenly distributed values in a given period interval. Results for the runs from June 17 and June 22 are shown in Fig. 7 and Fig. 8 (left side). The higher the deviation the higher the variability with the specific period, i.e. we can determine the significant period and possible errors from the shape of the  $\chi^2$ -period-plot.

Now we can take a closer look at the light curve folded on the maximum  $\chi^2$  period. They are plotted for the 2

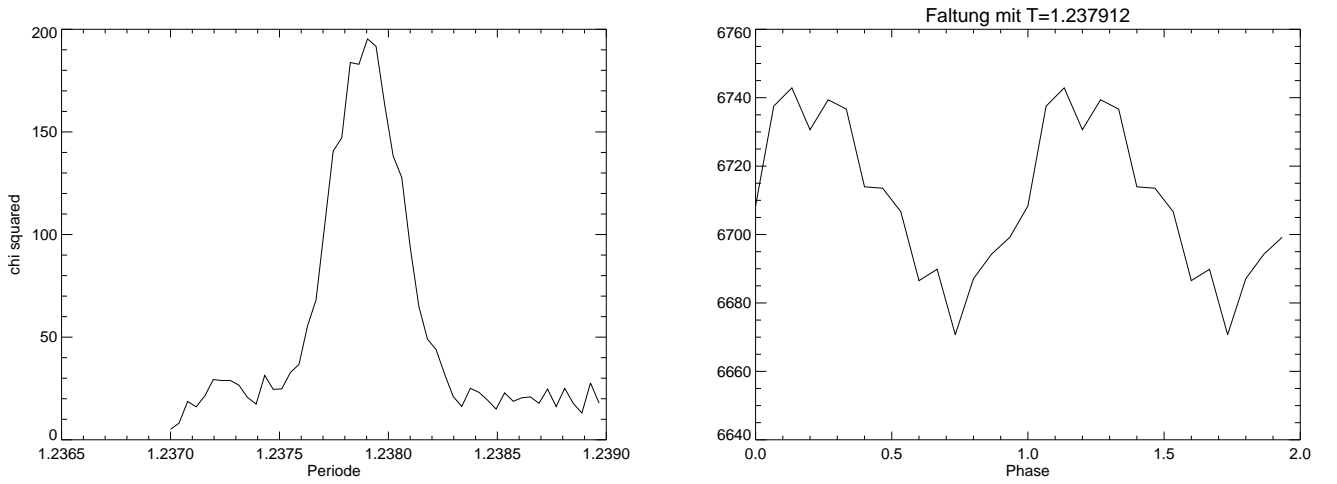


FIG. 7:  $\chi^2$ -period-plot for the epoch folding of the run from June, 17 (left) and light curve folded with the maximum  $\chi^2$  period (right)

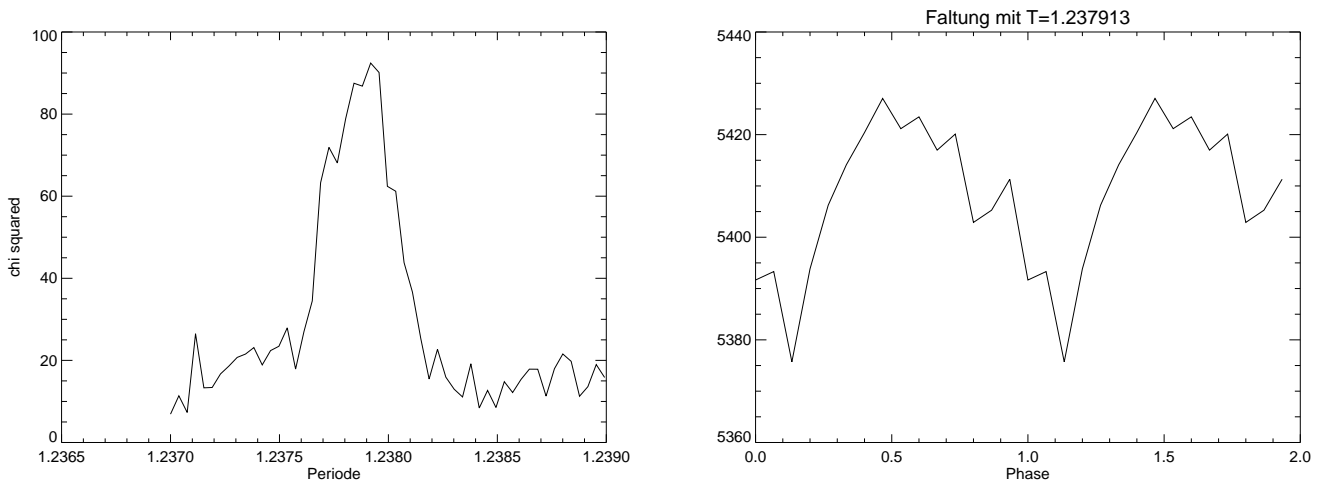


FIG. 8:  $\chi^2$ -period-plot for the epoch folding of the run from June, 22 (left) and light curve folded with the maximum  $\chi^2$  period (right)

runs mentioned above in Fig. 7 and Fig. 8 (right side). The curves do not only show the shape of the pulses, but we can also determine the *pulsed fraction*. We define this quantity as the ratio of the pulsed amplitude to the mean light level during the run. (This definition is different to the definition by [5], where the pulsed fraction is defined as the ratio of the pulsed amplitude to the *maximum* light level of HZ Her, i.e. at orbital phase 0.5).

In table II the results are summarized.

We can now estimate, where the pulsed radiation is emitted. We assume that we see the system edge on and that the orbit is circular. Hercules X-1 and HZ Herculis move in the  $x$ - $y$ -plane and the  $x$ -axis is pointing towards us, so the  $z$ -axis is parallel to the system's orbital angular velocity. The frequency of a pulsation emitted in

the plane will be Doppler-shifted, so we will detect the frequency

$$f = f_0 \left( 1 + \frac{\omega x}{c} \right). \quad (13)$$

$f_0$  is the pulsation frequency of the neutron star  $f_0 = 0.8078735 \text{ s}^{-1}$ . The orbital angular velocity is  $\omega = 4.2770 \times 10^{-5} \text{ Hz}$ .

The  $x$ -coordinate of the neutron star is given by

$$x_x = a \sin i \sin(2\pi p), \quad (14)$$

where  $p$  is the orbital phase. In Fig. 10 the Doppler shifted pulsation frequency of the neutron star and the observed optical pulsation frequencies are plotted versus orbital phase. The horizontal solid line indicates the mean spin frequency of Hercules X-1. The figure shows that the optical pulsation does not originate from the

TABLE II: Results from the Fourier analysis of the significant runs

Date of Run	Number of Run	Period	Orbital Phase	Pulsed Fraction
June 17	jun1702	1.237913(50) s	0.761(13)	$1.2 \pm 0.2$
June 19	jun1902	-	0.944(13)	$< 0.1$
June 19	jun1904	-	0.002(13)	$< 0.1$
June 20	jun2002	-	0.518(13)	$< 0.1$
June 20	jun2004	-	0.576(13)	$< 0.1$
June 21	jun2103	1.237639(80) s	0.167(13)	$0.9 \pm 0.2$
June 21	jun2104	1.237777(80) s	0.196(13)	$0.8 \pm 0.2$
June 22	jun2203	1.237912(50) s	0.699(13)	$1.0 \pm 0.2$
June 23	jun2305	-	0.373(13)	$< 0.1$

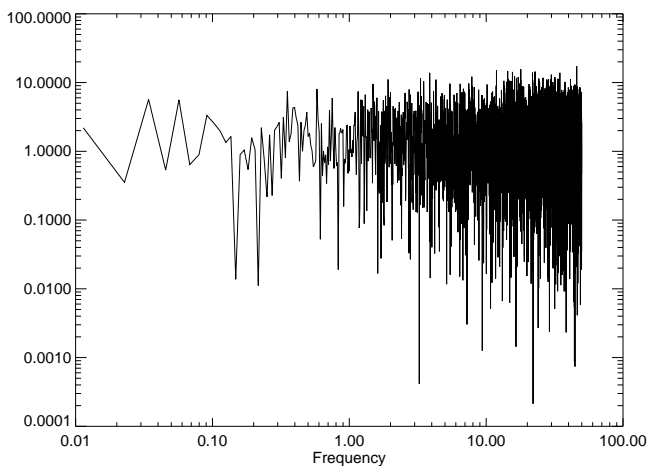


FIG. 9: PSD of the background from June 17

neutron star's accretion disc, since it is hardly Doppler-shifted. So the pulsation must come from a region, which is much closer to the center of mass of the binary, i.e. from the surface of HZ Herculis.

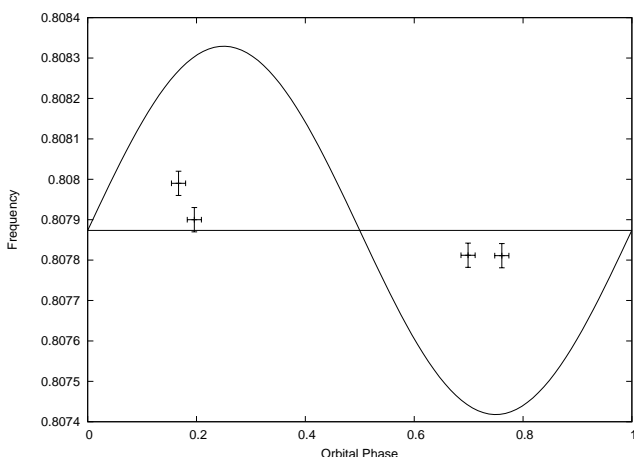


FIG. 10: The Doppler-shifted frequency of the neutron star and the observed frequencies plotted against phase

Another interesting feature that can be seen in Fig. 10 is that we observe pulsations only around orbital phase 0.20 and 0.75. That has also been shown by the long term observation of [5]. The fact that there is no pulsation at phase 0 (X-ray eclipse) is not astonishing, since we see the 'back' of the star, which is not hit by the X-ray pulses. But at first glance one would expect pulsations at phase 0.5, when the whole X-ray heated side of HZ Herculis is visible. In contrast neither our observations nor the ones by Middleditch *et al.* showed any events at phase 0.5.

In the next section I will present a geometrical model, which describes qualitatively many features of the observed behavior of the binary. Particularly it describes the dependence of the pulsed fraction on the orbital phase.

## V. GEOMETRICAL X-RAY REFLECTION MODEL

### A. Calculation Method

The model, which is described here, allows us to calculate the time dependence of the optical flux obtained from HZ Herculis. Since reprocessing of X-rays in stellar atmospheres is a very complex field, we will not deal with the exact mechanisms in this project. In our simulation we assume that the whole X-ray flux incident on the surface of HZ Herculis is immediately reprocessed to optical wavelength and reflected (Similar theoretical treatments of the X-ray reprocessing have been made by Middleditch and Nelson [5] and Chester [7], [8]).

We first have to take a look at the geometry of the system (See FIG. 11). Due to the presence of the neutron star and its gravitational field HZ Herculis doesn't have a spherical shape. The surface is a Roche equipotential, i.e. the gravitational potential

$$V_{pot}(\vec{r}) = G \left( \frac{M_x}{|\vec{r}|} + \frac{M_{opt}}{|\vec{r} - \vec{r}'|} \right) \quad (15)$$

is constant on the surface of HZ Herculis ( $\vec{r}'$  is the vector, that connects the 2 stars). The results is a tear-drop

shaped star.

Instead of applying the exact form of the Roche equipotential we make an approximation. Therefore we assume that HZ Herculis fills its Roche lobe, i.e. the surface of the star extends to the Lagrangian point L1. That's the point where the contributions to the gravitational force of the two stars exactly cancel.

From the mass ratio  $M_{opt}/M_x = 1.533$  and the semi-major axis  $a \cdot \sin i = 13.19$  s (we assume  $i = 90^\circ$ ) we can immediately calculate the distance of the two stars:

$$r' = a + \frac{M_x}{M_{opt}}a = 6.537 \times 10^9 \text{ m}. \quad (16)$$

With the balance of forces

$$\frac{GM_{opt}}{\rho_{max}^2} = \frac{GM_x}{(r' - \rho_{max})^2} \quad (17)$$

we calculate the distance from L1 to the center of HZ Herculis as  $\rho_{max} = 3.616 \times 10^9$  m and the distance from L1 to Hercules X-1 as  $d = r' - \rho_{max} = 2.921 \times 10^9$  m.

Near the Lagrange point the Roche lobe has a cone like structure. So we approximate the Roche equipotential by a second order polynomial  $r(\rho) = \beta\rho \left(1 - \frac{\delta\rho}{R}\right)$ , where  $\rho$  is the distance from the Lagrange point and  $r$  the radius of the cone. The two parameters  $\beta$  and  $\delta$  are given by the constraints

$$\begin{aligned} r(\rho_{max}) &= R = 2.923 \times 10^9 \text{ m} \\ r'(\rho_{max}) &= 0. \end{aligned} \quad (18)$$

So in our case  $\beta = 1.617$  and  $\delta = 0.404$ .

For the 'back' of the star (the side, that is not heated by X-rays) we assume a spherical structure with radius  $R$ , i.e. we neglect the gravitational field of the neutron star. So the profile of the star is given by the function

$$r(\rho) = \begin{cases} \beta\rho \left(1 - \frac{\delta\rho}{R}\right) & , \rho \leq \rho_{max} \\ R\sqrt{1 - (\rho - \rho_{max})/R} & , \rho_{max} < \rho < \rho_{max} + R \end{cases} \quad (19)$$

After having defined the shape of the star we can now proceed to calculate the optical flux observed. The flux consists of two components. The first one is the optical luminosity of the star itself ( $I_{opt}$ ), which is constant over the whole surface of the star, the second is due to the X-rays, that hit the surface of HZ Herculis and are reprocessed to optical wavelength ( $I_x$ ).

$$I(t) = I_{opt} + I_x(t) \quad (20)$$

So  $I_{opt}$  is given by the integral

$$I_{opt} = \int_S ds P(\hat{n}, \hat{n}') \frac{L_{opt}}{4\pi R^2}, \quad (21)$$

where  $\hat{n}$  is the normal vector at  $ds$  and  $\hat{n}'$  is the unit vector towards the observer.  $P(\hat{n}, \hat{n}')ds = (\hat{n} \cdot \hat{n}')ds$  is the projection of the surface element onto the field of

vision of the observer (i.e. the fraction of the area that is visible from earth). We set  $P(\hat{n}, \hat{n}')$  to zero for  $\hat{n} \cdot \hat{n}' < 0$ , i.e. the surface element is not visible from earth.  $L_{opt}$  is the constant luminosity of HZ Herculis.

Now we have to investigate the second term in (20).

$$I_x(t) = \int_S ds P(\hat{n}, \hat{n}') P(-\hat{m}, \hat{n}) \frac{L_x(t)}{4\pi l^2}, \quad (22)$$

where  $l = \sqrt{(d + \rho)^2 + r^2}$  is the distance of the surface element  $ds$  to the neutron star and  $\hat{m}$  is the unit vector from Hercules X-1 to the surface element. The second projection term  $P(-\hat{m}, \hat{n}) = -\hat{m} \cdot \hat{n}$  gives the visible area of HZ Herculis from the neutron star.

$L_x(t)$  is the X-ray luminosity of Hercules X-1. We set the mean luminosity  $\langle L_x \rangle = 1$ . Besides we assume that 50% of the X-ray flux is pulsed and we approximate the X-ray pulse profile by a sine function with frequency  $f_0 = 0.8078735$  Hz. So we can write

$$L_x(t) = (1 + 0.5 \sin(2\pi f_0(t - \Delta x/c))). \quad (23)$$

$\Delta x/c$  gives the time of flight difference of the emitted pulses for the different surface elements. Let  $\Delta x = 0$  for  $\vec{r} = (0, 0, 0)$  (the apex of the cone), then we can express the runtime difference for the surface element at  $\vec{r}$  to the observer by

$$\Delta x = \sqrt{(d + \rho)^2 + r^2} - d - \hat{n} \cdot \vec{r} \quad (24)$$

We still have to determine the optical luminosity of HZ Herculis  $L_{opt}$ . According to the observations the luminosity at phase 0 is about 1.5 magnitudes lower than at orbital phase 0.5. To obtain a similar result for our model we let  $L_{opt} = 0.00436$ .

In the numerical calculation of the model 10<sup>6</sup> supporting points were used to specify the surface of HZ Herculis. The calculation was performed for 50 equally spaced observation angles between 0 and  $\pi$ , which correspond to orbital phase 0.5 to 1. Since the model is symmetric we can immediately give the observed flux for the phase 0 to 0.5.

## B. Results

The model described above allows us to calculate the pulsed fraction as a function of orbital phase. We define the pulsed fraction as the ratio of the pulsed amplitude to the mean light level. The result is shown in Fig. 12, besides the calculated mean luminosity is shown in Fig. 13. The pulsed fraction vanishes for orbital phase 0 and 1 respectively, since we do not see any reprocessed X-ray radiation. Besides the model predicts almost no pulsation in the optical flux at phase 0.5. This feature is in entire agreement with the observation, since neither our observation nor the long-term observation by Middleditch & Nelson [5] showed significant variability at orbital phase 0.5. The result of their observation is



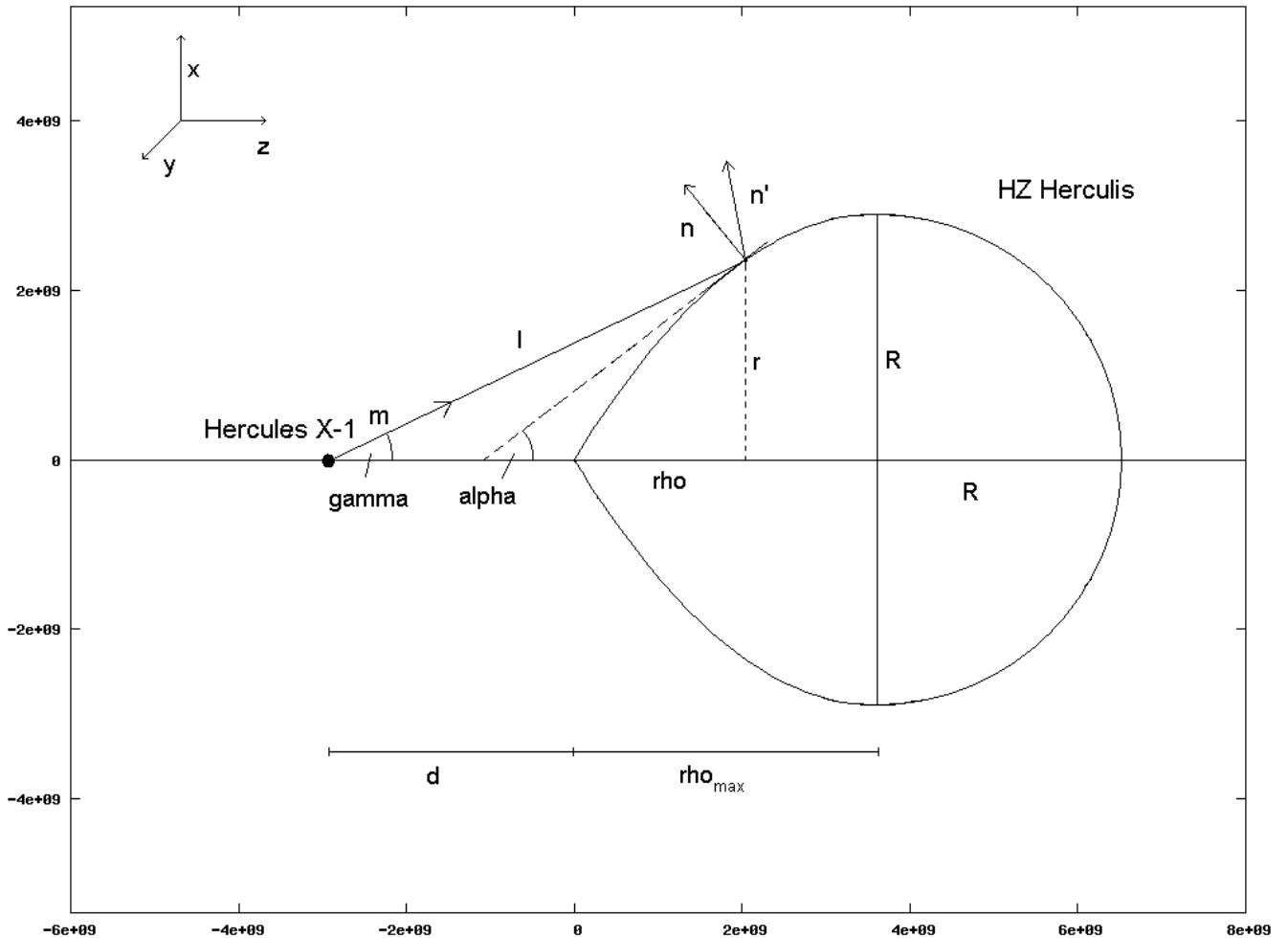


FIG. 11: Geometry of the reflection model

shown in Fig. 14. Instead the calculated pulsed fraction has peaks at phases 0.15 and 0.25 (0.85 and 0.75 respectively). As one can see in Fig. 14, Middleditch & Nelson found that the pulsed fraction has its maximum between orbital phase 0.20 and 0.25 (0.75 and 0.80 respectively), which is in good agreement with our results from the purely geometrical model. So the model also explains why only 4 lightcurves in our observation showed variability. Those significant light curves were recorded around orbital phase 0.2 and 0.75, in contrast most of the light curves, that did not show variability, were recorded around orbital phase 0 and 0.5 (see table II).

The peak value in Fig. 12 is about 8%. This is much higher than the observed pulsed fractions (see table II). The difference is due to the approximations we made in our reflection model. We assumed that the *total* X-ray flux is *immediately* reflected in the optical regime. In reality only a small fraction of the incoming X-rays are reprocessed into the optical. This leads to an overall efficiency factor in front of the X-ray integral in equation

(20). Besides the X-rays are reprocessed with a mean finite reprocessing time  $t_r$ . Statistical fluctuations of the reprocessing time lead to additional contributions to the runtime difference. But, since  $t_r$  is much smaller than the pulse period, the influence of the finite reprocessing time is negligible.

## VI. CONCLUSION

We can now summarize the results obtained from our optical observation and the geometrical calculation in the last section.

The observation showed weak optical pulsations at a frequency near the pulsation frequency of Hercules X-1. The fact that the frequency is hardly Doppler-shifted indicates that the pulses originate from the surface of HZ Herculis and not from the neutron star's accretion disc. Furthermore we found that the presence of pulsations and the amount of pulsed light is correlated with the orbital

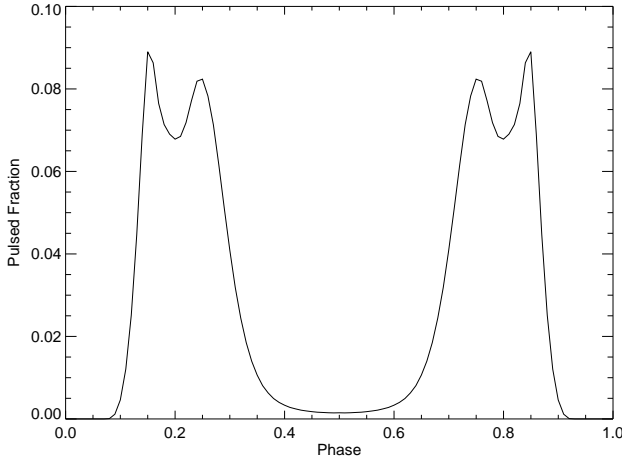


FIG. 12: Geometrical reflection model: pulsed fraction versus orbital phase

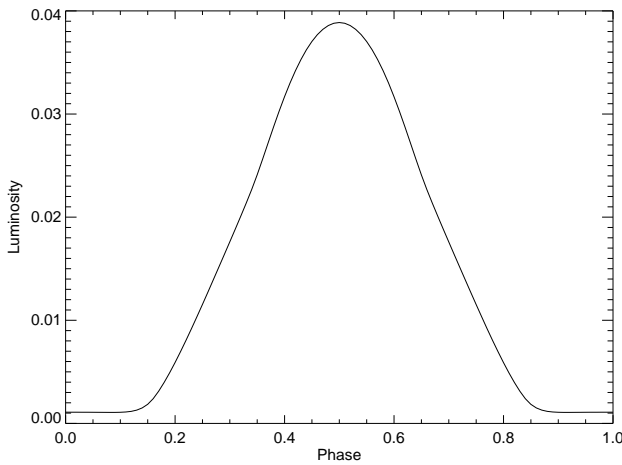


FIG. 13: Geometrical reflection model: mean luminosity ( $L/L_x$ ) versus orbital phase

phase of the binary. This feature explains why only 4 of the approximately 50 runs show variability. All in all we successfully confirmed the results from the seventies by Davidsen and Middleditch *et al.* on optical pulsations in the light curve of HZ Herculis.

For a better understanding of the correlation of the pulsed fraction with the orbital phase we constructed a geometrical model of the binary. The model was used to calculate the optical flux emitted by HZ Herculis by assuming that the whole X-ray flux is immediately reprocessed to optical wavelength on the surface of the star. The results from the numerical calculation are quite consistent with the observations. The model yields the right dependence of the pulsed fraction on the orbital phase. But to obtain more accurate values for the pulsed frac-

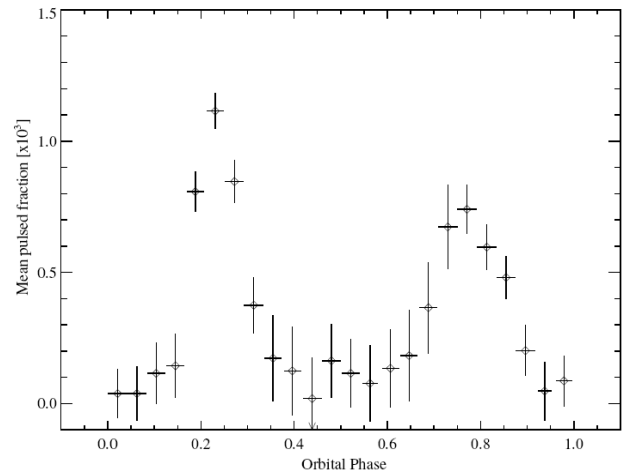


FIG. 14: Pulsed fraction versus orbital phase from the observation by Middleditch and Nelson 1976

tion one would also have to take into account the exact physical process of the X-ray reprocessing.

- 
- [1] Press, W. H., Teukolsky, S. A., Vetterling, W. T., and Flannery, B. P. *Numerical Recipes in Fortran* (Cambridge University Press, 1986).
  - [2] Kuster, M., 2004, Dissertation, Universität Tübingen
  - [3] Davidsen, A., Henry, J. P., Middleditch, J., and Smith, H. E. 1972, *Ap. J. (Letters)*, **177**, L97
  - [4] Davidsen, A., Margon, B., and Middleditch, J. 1975, *Ap. J.*, **198**, 653
  - [5] Middleditch, J., and Nelson, J. E. 1976, *Ap. J.*, **208**, 567
  - [6] Middleditch, J., Pennypacker, C. R., and Burns, M. S. 1983, *Ap. J.*, **274**, 313
  - [7] Chester, T. J. 1978, *Ap. J.*, **222**, 652
  - [8] Chester, T. J. 1978, *Ap. J.*, **227**, 569
  - [9] Leahy, D. A., Darbro, W., Elsner, R. F., Weisskopf, M. C., Kahn, S., Sutherland, P. G., and Grindlay, J. E. 1983, *Ap. J.*, **266**, 160